Cell adhesion presence during adolescence controls the architecture of projection-defined prefrontal cortical neurons and reward-related action strategies later in life

Henry W. Kietzman [a,b,c,d], Lauren P. Shapiro [b,d,e], Gracy Trinoskey-Rice [b,d], Shannon L. Gourley [b,c,d,e,f,*]

[a] Medical Scientist Training Program, Emory University School of Medicine, United States
[b] Departments of Pediatrics and Psychiatry, Emory University School of Medicine, United States
[c] Graduate Program in Neuroscience, Emory University, United States
[d] Yerkes National Primate Research Center, Emory University, United States
[e] Graduate Program in Molecular and Systems Pharmacology, Emory University, United States
[f] Children's Healthcare of Atlanta, United States

ARTICLE INFO

ABSTRACT

Adolescent brain development is characterized by neuronal remodeling in the prefrontal cortex; relationships with behavior are largely undefined. Integrins are cell adhesion factors that link the extracellular matrix with intracellular actin cytoskeleton. We find that β1-integrin presence in the prelimbic prefrontal cortex (PL) during adolescence, but not adulthood, is necessary for mice to select actions based on reward likelihood and value. As such, adult mice that lacked β1-integrin during adolescence failed to modify response strategies when rewards lost value or failed to be delivered. This pattern suggests that β1-integrin-mediated neuronal development is necessary for PL function in adulthood. We next visualized adolescent PL neurons, including those receiving input from the basolateral amygdala (BLA) – thought to signal salience – and projecting to the dorsomedial striatum (DMS) – the striatal output by which the PL controls goal-seeking behavior. Firstly, we found that these projection-defined neurons had a distinct morphology relative to general layer V PL neurons. Secondly, β1-integrin loss triggered the overexpression of stubby-type dendritic spines at the expense of mature spines, including on projection-defined neurons. This phenotype was not observed when β1-integrins were silenced before or after adolescence. Altogether, our experiments localize β1-integrin-mediated cell adhesion within a developing di-synaptic circuit coordinating adaptive action

1. Introduction

Neurodevelopment during adolescence is characterized by dramatic structural plasticity within the prefrontal cortex (PFC), involving both the elimination of dendritic spines and the stabilization of remaining spines (Crews et al., 2007; Spear, 2000). Early-life development is the subject of intense investigation, but mechanisms underlying adolescent brain development are still unclear – even despite ~50% of "adult" mental health disorders initially presenting during adolescence (Kessler et al., 2007). Further, structural irregularities in the PFC are linked to the cognitive symptomatology of nearly every major neurodevelopmental disorder (Penzes et al., 2011; Glausier and Lewis, 2013; MacDonald et al., 2017). Thus, investigating factors that govern

structural stability – referring here to the process by which dendritic spines are retained and escape pruning – is a crucial step in understanding neurodevelopment during adolescence and potentially, disease etiologies.

Integrins are heterodimeric transmembrane cell adhesion receptors that provide a link between the extracellular matrix (ECM) and the intracellular actin cytoskeleton. Integrins, composed of a ligand-binding α subunit and a β subunit that activates intracellular signaling cascades, respond to ECMs, either to maintain structural integrity and functionality, or to promote tissue differentiation and development (Humphrey et al., 2014). In early life, β1-subunit-containing integrin receptors promote neurite outgrowth (Ivankovic-Dikic et al., 2000) and axon guidance (Pasterkamp et al., 2003). Investigations focused on

hippocampal CA1 suggest that during adolescence, β1-integrins may fulfill a distinct function: stabilizing dendrites and synapses (Warren et al., 2012), thereby supporting long-term potentiation (Kramár et al., 2006). Levels of the neuronal β1-integrin signaling partners, p190Rho-GAP and Rho-kinase 2 (ROCK2), peak in the PFC during adolescence, suggesting that β1-integrin-mediated signaling in adolescence might stabilize PFC neuron structure and function (Shapiro et al., 2017).

Broadly, the PFC, and the prelimbic subregion (PL) in particular, controls adaptive action, referring here to the ability of organisms to link actions with their likely outcomes and to modify behaviors when contingencies change (Woon et al., 2020; Balleine and O'Doherty, 2010). We report here that β1-integrin presence in the PL during adolescence, but not later, controls action strategy selection in adulthood. As such, mice deficient in developmental β1-integrins during adolescence later struggle to: **1)** link actions with outcomes and **2)** select actions based on outcome value. These behaviors require coordinated limbic-frontal-striatal circuits (Balleine and O'Doherty, 2010). We thus characterized the dendritic micro-architecture of adolescent layer V PL neurons receiving input from the basolateral amygdala (BLA) – responsible for salience detection – and projecting to the dorsomedial striatum (DMS), the primary striatal output necessary for goal-oriented action (Hart et al., 2014). Surprisingly, these projection-defined neurons had a more "adult-like" morphology relative to a general population of layer V PL neurons. β1-integrin loss caused the overexpression of stubby-type dendritic spines in this subpopulation, which are unlikely to contain synapses, at the expense of mature spine types. Together, these experiments indicate that β1-integrin presence during adolescence structurally stabilizes PL neurons positioned within a di-synaptic circuit, likely providing the structural substrates for adaptive decision making later in life.

2. Results

2.1. Cell adhesion during adolescence optimizes action strategies in adulthood

We aimed to understand the function of β1-integrins in the developing postnatal PFC. To reduce β1-integrins, we introduced a CaMKIIα-driven adeno-associated viral vector (AAV) expressing Cre recombinase (Cre) into the PL of transgenic *Itbg1^{tm1Efu}* (*Itgb1*-flox) mice. These mice have loxP sites flanking exon 3 of *Itgb1*, the gene that encodes β1-integrins; Cre introduction deletes this exon (Raghavan et al., 2000). Cre was delivered early in life, to reduce β1-integrins starting in adolescence, or for comparison, in adulthood (infusions at P21–24 or P56–60, respectively; ages and viral vector details for all experiments are described in Table 1). Fig. 1a depicts viral vector transfection, comparable across ages; any mice with unilateral or off-target transfection were excluded.

Viral-mediated *Itgb1* silencing significantly reduced β1-integrin protein levels in gross tissue punches in adolescence [one-sample t-test compared to 1 (full β1-integrin content): $t_{(5)} = 5.118$, $p = 0.0037$] and adulthood [one-sample t-test compared to 1 (full β1-integrin content): $t_{(3)} = 3.346$, $p = 0.044$] (Fig. 1b), with no significant difference between the two groups [$t_{(8)} = 1.889$, $p = 0.097$]. Values were also comparable to prior experiments using the same strategy (DePoy et al., 2019). In those experiments, protein levels were measured at a later time point, suggesting that the degree of protein loss is stable beyond an initial viral vector incubation period. These patterns are consistent with evidence that AAVs reach peak expression 2–3 weeks following delivery and then express for several months (Ahmed et al., 2004). Note that incomplete protein loss was expected, given that tissue punches processed by western blot contained both transduced and unaffected tissues, and CaMKIIα-driven AAVs would be expected to spare glial β1-integrins, which are expressed at high levels (Cahoy et al., 2008). (Western blot was used because immunostaining brain tissue with currently-available antibodies is quite difficult.) Figures depict group means and individual

Table 1
Genotype, age, and viral vector details for all experiments.

Fig.	Geno-type of mice	Timing of viral vector delivery	Viral vector conditions	Measure
1a, 2, S1, S2	*Itgb1*-flox	P21–24 vs. > P56	*Knockdown*: AAV2/8-CaMKIIα-mCherry+Cre *Control*: AAV2/8-CaMKIIα-mCherry	Test for decision making capacity
1b–c	*Itgb1*-flox	P21–24 vs. > P56	*Knockdown*: AAV2/8-CaMKIIα-mCherry+Cre *Control*: AAV2/8-CaMKIIα-mCherry	Immuno-blotting for β1-integrins
3, S3	*Itgb1*-flox/ *Thy1*-YFP	P21–24 vs. > P56	*Visualization of projection-defined PL neurons*: rgAAV-hSyn-DIO-mCherry (DMS) AAV1-hSyn-Cre-WPRE-hGH (BLA) *Visualization of general layer V populations*: AAV2/8-CaMKIIα-mCherry	Dendritic spine analysis
4, S3, S4	*Itgb1*-flox/ *Thy1*-YFP	P21–24 vs. > P56–60	*Adolescent Itgb1 knockdown in projection-defined neurons*: rgAAV-hSyn-DIO-mCherry (DMS) AAV1-hSyn-Cre-WPRE-hGH (BLA) *Adolescent projection-defined control neurons*: rgAAV-hSyn-DIO-mCherry (DMS) AAV1-hSyn-Cre-WPRE-hGH (BLA) *Adolescent- or adult-onset Itgb1 knockdown in general layer V neurons*: AAV2/8-CaMKIIα-mCherry + Cre *Adolescent- or adult-onset general layer V control neurons*: AAV2/8-CaMKIIα-mCherry *Embryonic-onset Itgb1 knockdown was achieved viral non-viral methods described in text*	Dendritic spine analysis

mice.

β1-integrin activation results in the phosphorylation of p190RhoGAP (Bradley et al., 2006). β1-integrin protein levels correlated with the proportion of phospho-p190RhoGAP/p190RhoGAP in knockdown mice, such that mice with fewer β1-integrins also had the less phospho-p190RhoGAP [$r^2 = 0.49$, $p = 0.036$] (Fig. 1c), evidence that our gene silencing approach had functional consequences for integrin-mediated intracellular signaling.

The PL is necessary for mice and rats to use associations between actions and outcomes to guide choice behavior (Woon et al., 2020). To understand whether β1-integrins in adolescence are necessary for this function in adulthood (i.e., to determine whether β1-integrins equip developing mice with the capacity for adaptive behavior in adulthood), we reduced β1-integrins in adolescence and tested decision-making capacity in adulthood. For comparison, we also reduced β1-integrin presence in adulthood. Control mice with control viral vectors delivered in adolescence or adulthood did not differ and were combined. Mice were trained to nose poke at 2 apertures for 2 distinct food reinforcers (Fig. 2a). Groups did not differ in response acquisition, with mice increasing responding over time [main effect of day ($F_{(6,246)} = 25.53$, $p < 0.0001$), no day*group interaction or other main effects ($Fs < 1$)] (Fig. 2b). There were no systematic preferences for either flavor of pellet that would affect subsequent phases of testing (Fig. S1), so response rates for both pellets are collapsed for simplicity. Further, there were no differences in food magazine entries between groups during training (Fig. S1).

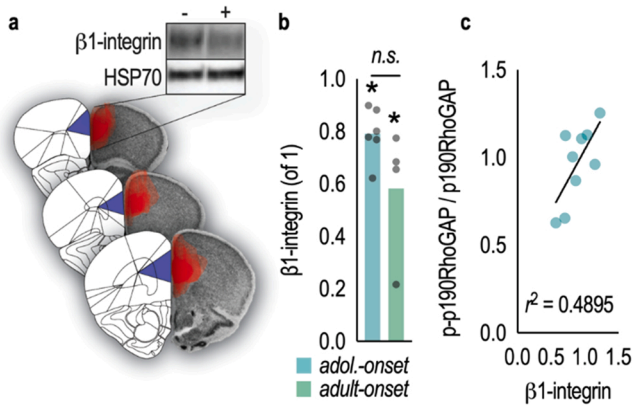Next, the contingency between 1 familiar action and its outcome was

Fig. 1. *Itgb1* **knockdown reduces β1-integrin protein levels. a.** CaMKII-AAVs containing Cre were infused bilaterally into PL of *Itgb1*-flox mice. (**left**) Images from Allen Brain Atlas (from left: + 2.71 mm, + 2.22 mm, and + 1.98 mm relative to bregma) depicting the PL (purple). (**right**) Overlays of viral vector spread (red) encompassing the PL from mice in this report on images from the Mouse Brain Library (Rosen et al., 2000). All cohorts exhibited consistent viral vector localization. (**top right**) Representative blots. **b.** Viral-mediated *Itgb1* silencing significantly reduced β1-integrin protein levels in PFC tissue punches from both adolescents and adults. Incomplete protein loss was expected, given that samples contained transduced and unaffected cells, and glial integrins were spared. There were no age-based differences in β1-integrin levels. **c.** β1-integrin protein levels correlated with phosphorylation (activation) of the neuronal substrate p190RhoGAP. Bars represent means, and symbols represent individual mice. *$p < 0.05$ relative to 1.0; "n.s." refers to no significant difference between ages; "adol." refers to "adolescent.

violated by providing pellets non-contingently, or "for free," and responding was not reinforced. Response and pellet delivery rates during this "non-contingent" session did not differ between groups (Fig. S1). Subsequently, control mice inhibited that response during a probe test, preferring instead the response associated with the intact contingency. Meanwhile, loss of β1-integrins starting in adolescence, but not adulthood, ablated this preference [group*aperture interaction ($F_{(2,41)}$ = 6.810, $p = 0.0028$), main effect of aperture ($F_{(1,41)}$ = 47.99, $p < 0.001$), main effect of group ($F_{(2,41)} = 4.593$, $p = 0.016$)] (Fig. 2c). This effect was not sex-dependent (Fig. S2). Thus, developmental integrins are necessary for the ability of mature mice to learn about action-outcome relationships and thus favor behaviors that are likely to be reinforced.

Adaptive action involves selecting actions based on the value of likely outcomes (Woon et al., 2020). Thus, we hypothesized that developmental β1-integrins would also be necessary for mice to select actions based on outcome value, which we tested using satiety-specific devaluation (Fig. 2d). Following training, mice were allowed to freely consume 1 of the 2 food reinforcers (grain or chocolate) in a separate environment, decreasing the value of that reinforcer. Groups did not differ in food consumption [$F < 1$] (Fig. 2e). Control mice preferentially responded for the other, "valued" food when returned to the operant conditioning chambers, evidence that they selected actions based on outcome value. Meanwhile, reducing β1-integrins in adolescence, but not adulthood, blocked the ability of adult mice to select actions based on outcome value [group*value interaction ($F_{(2,21)} = 3.451$, $p = 0.05$), main effect of group ($F_{(2,21)} = 3.457$, $p = 0.05$), main effect of value ($F_{(1, 19)} = 4.738$, $p = 0.04$)] (Fig. 2f). Thus, β1-integrin expression during adolescence, but not adulthood, is required for selecting actions based on outcome value.

2.2. Developmental β1-integrins are necessary for the morphological features of PL neurons positioned within a BLA-PL-striatal circuit

β1-integrins are largely localized in the post-synapse of excitatory

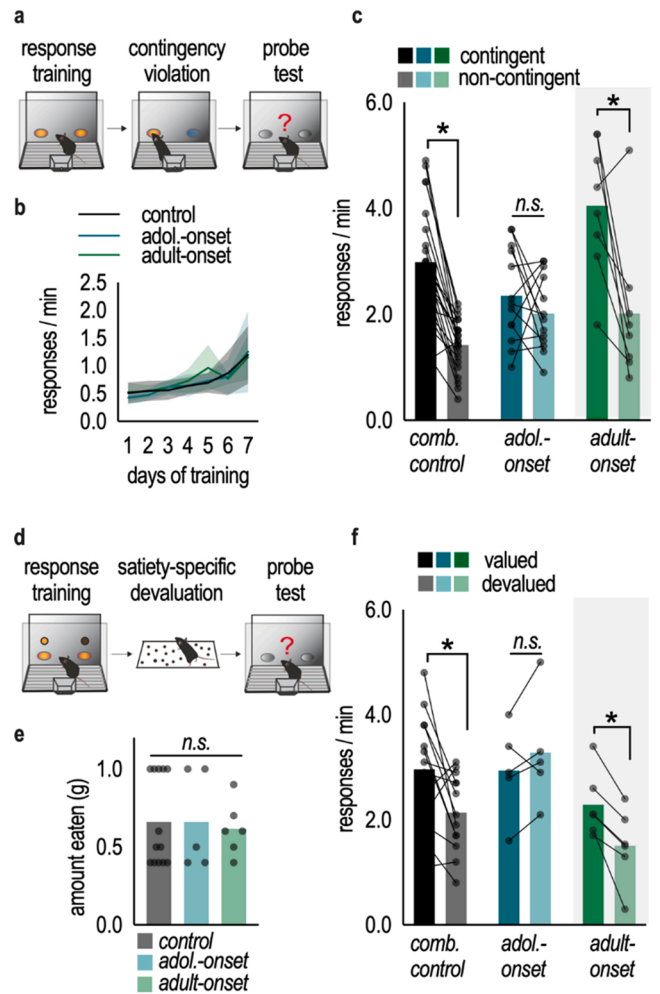**Fig. 2. Developmentally-selective control of action selection by cell adhesion factor β1-integrin. a.** Schematic. Mice are trained to nose poke at 2 apertures for 2 food reinforcers. Once mice are proficient, the causal relationship between 1 behavior and its outcome is violated, and response preference is later tested. **b.** Groups did not differ in response training. There were no systemic preferences for either flavor of pellet, so response rates for both pellets are collapsed here **c.** Control mice subsequently inhibited a behavior that was not reinforced and favored a reinforced behavior, but reduction of β1-integrins starting in adolescence ablated response preference. Adult-onset loss had no effects. **d.** Schematic. Mice are trained to nose poke at 2 nose poke apertures for 2 food reinforcers. Once proficient, mice are then allowed to freely consume 1 of the 2 food reinforcers in a separate environment. In a subsequent probe test, preferential responding for the other food ("valued" condition) is considered "goal-directed". **e.** Groups did not differ in food consumed during the pre-feeding session. **f.** Control mice preferred the aperture associated with the valued food reinforcer, whereas adolescent-onset, but not adult-onset, loss of β1-integrins ablated this preference. Bars represent means, error bars represent SEMs, and symbols represent individual mice. *$p < 0.05$. "Comb." refers to "combined," and "adol." refers to "adolescent".

synapses in the postnatal brain, coordinating the stability of these synapses (Schuster et al., 2001; Mortillo et al., 2012). Thus, it seems likely that reducing *Itgb1* during adolescent development disrupts the ability of mature PL neurons to effectively receive inputs necessary for adaptive behavior. One candidate region is the BLA, given that BLA→PL projections develop throughout adolescence (Cunningham et al., 2002); this development ensures that connections required for certain goal-seeking behaviors are accessible in adults (Wassum and Izquierdo, 2015; Fisher et al., 2020). We thus hypothesized that β1-integrin presence sculpts the development of PL neurons receiving input from the BLA. Cortically-oriented BLA projections terminate on layer II, III, and V PL

neurons (Cheriyan et al., 2016). We focus here on layer V neurons because these cells receive input from the BLA and send outputs to the dorsomedial striatum (DMS), which is required for the translation of decision making into action (Hart et al., 2018a, 2018b).

It was first necessary to isolate and characterize PL neurons receiving inputs from the BLA and projecting to the DMS under typical (β1-integrin+) conditions. We isolated projection-defined PL neurons by infusing an anterograde transsynaptic Cre-expressing viral vector into the BLA and a retrograde Cre-dependent mCherry-expressing viral vector into the DMS of adolescent *Thy1*-YFP^H mice (Feng et al., 2000) (Fig. 3a–b). Thus, mCherry+, YFP+ co-labeled cells represent layer V neurons that receive projections from the BLA, and project to the DMS (Fig. 3c). For comparison, we infused an mCherry-expressing viral vector into the PL of adolescent and adult mice, allowing us to visualize a general population of transduced layer V neurons not defined by projection (Fig. 3d). As above, viral vectors were infused at P21–24 or P56–60, and mice were euthanized 3 weeks later (Fig. 3e). We then utilized high-resolution imaging and 3D dendritic spine reconstruction to analyze the dendritic micro-architecture of each population.

Interestingly, projection-defined PL neurons had lower dendritic spine densities than either adult or adolescent undefined PL layer V populations (Fig. S3). To account for these differences, we focused here on the proportions of mature and immature spine subtypes, given that the balance between mature vs. immature spine subtypes allows for the

prioritization and integration of certain inputs over others (Holtmaat et al., 2005). The proportion of immature, stubby-shaped dendritic spines was highest in adulthood and lowest in adolescence, and projection-defined neurons had an intermediate phenotype, indistinguishable from both groups [$F_{(2,17)} = 3.914$, $p = 0.04$] (Fig. 3f,g). Projection-defined neurons had a lower proportion of mature, mushroom-shaped dendritic spines than the general population of adolescent neurons, more closely resembling adult neurons, although this comparison did not reach statistical significance [$F_{(2,17)} = 3.115$, $p = 0.0704$] (Fig. 3f, g). Thin-type spine proportions did not differ between groups [$F_{(2,17)} = 1.806$, $p = 0.19$] (Fig. 3f, g).

We next characterized the morphological features of each dendritic spine subtype. Mushroom-type spines on projection-defined neurons again more closely resembled adult spines in length than same-age counterparts collected from a general layer V population [$F_{(2,17)} = 8.578$, $p = 0.003$] (Fig. 3h). Spine diameters did not differ [$F < 1$] (Fig. 3h). Interestingly, spine volume was largest in adult mice [$F_{(2,17)} = 74.37$, $p \leq 0.0001$] (Fig. 3i). Thus, the morphology of mushroom-shaped spines on projection-defined neurons in some ways resembled adult spines (in length), and in some ways resembled their undefined adolescent counterparts (in volume).

We identified a similar pattern for stubby-shaped spines, in that stubby-type spines on projection-defined neurons exhibited decreased spine length [$F_{(2,17)} = 6.036$, $p = 0.01$] and diameter [$F_{(2,17)} = 15.94$,
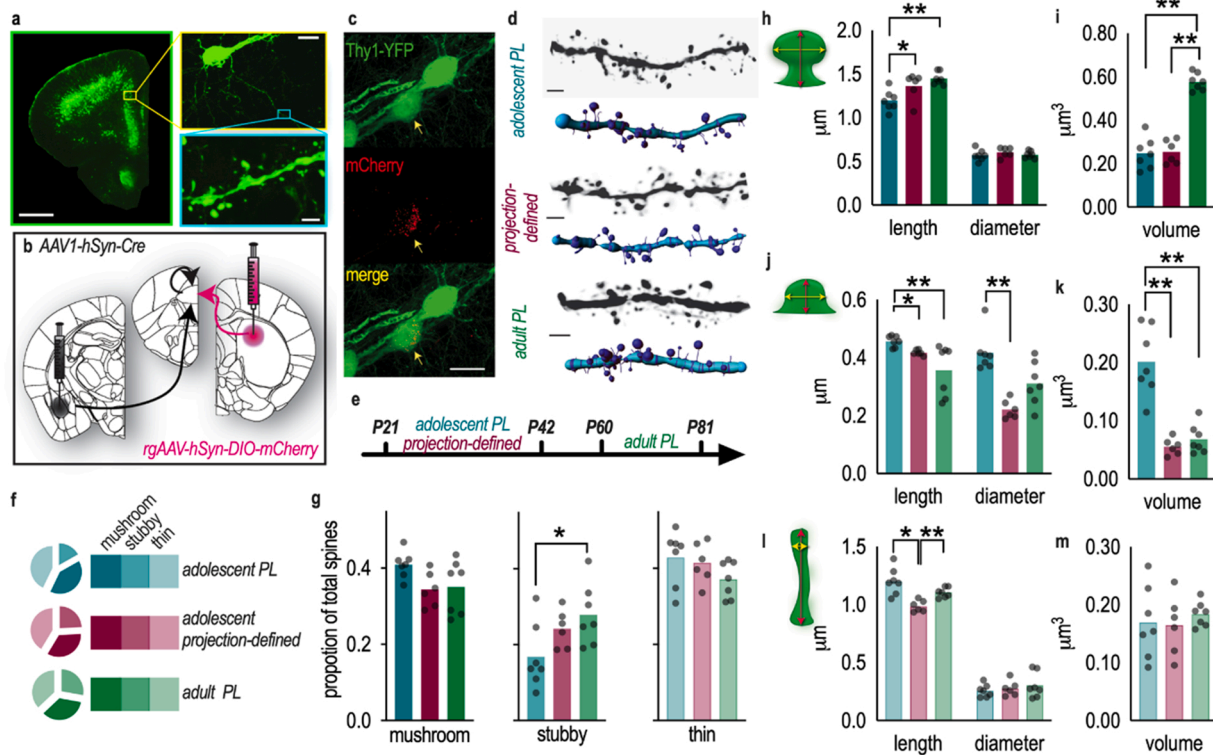

Fig. 3. **Morphological features of PL neurons receiving input from the BLA and projecting to the DMS. a.** Coronal sections from *Itgb1+/Thy1*-YFP mice used to examine dendritic spine architecture on excitatory layer V PL neurons. Scale bar= 1 mm (green), 20 μm (yellow), 2 μm (blue). **b.** Schematic of viral vector approach. A retrograde viral vector expressing a Cre-dependent fluorophore was infused into the DMS. A transsynaptic anterograde viral vector encoding Cre was infused into the BLA. Mice were YFP+. Separate mice received an AAV-mCherry to label a general neuron population not defined by projection pattern. **c.** Representative PL neuron co-expressing YFP and mCherry (arrowhead). Scale bar = 20 μm. **d.** Representative dendrites, with their associated 3D reconstructions. Scale bar = 2 μm. **e.** Timeline of experiments portraying time of viral vector delivery and euthanasia. **f.** Pie charts representing the dendritic spine subtype proportions in each group. **g.** Mature neurons had the highest proportion of stubby-type spines, while projection-defined neurons exhibited an intermediate phenotype. There were no significant differences in the proportions of mature- or thin-type spines. **h.** Projection-defined adolescent PL neurons had longer mushroom-type spines than the general adolescent population, resembling mature morphologies. We observed no differences in dendritic spine diameters. **i.** Mature neurons had mushroom-shaped spines of the largest volume, exceeding both adolescent populations. **j.** Projection-defined adolescent PL neurons and mature PL neurons had shorter stubby-type spines than the general population of adolescent PL neurons. Projection-defined adolescent PL neurons and mature neurons had smaller stubby-type spine diameters than the general adolescent population. **k.** Their volumes were also lower. **l.** Projection-defined adolescent PL neurons had shorter thin-type spines than other groups, and there were no differences in thin spine diameters, or **m.** thin spine volumes. Bars represent means, and symbols represent individual mice. *$p < 0.05$, **$p < 0.001$.

$p = 0.0001$] compared to the general population of same-age spines and more closely resembled adult spines (Fig. 3j). Stubby-type spine volume was similar in adult and projection-defined adolescent populations, and far lower than a general adolescent population [Welch's ANOVA $W_{(2,10.19)} = 18.76$, $p < 0.0004$] (Fig. 3k).

Lastly, projection-defined adolescent neurons had shorter thin-type spines than other groups [$F_{(2,17)} = 12.28$, $p = 0.0005$], with no group differences in diameters or volumes [$Fs < 1$] (Fig. 3l, m). Thus, layer V PL neurons positioned within a BLA→PL→DMS circuit exhibit distinctive morphologies relative to a general population of layer V PL neurons.

We next asked: Do β1-integrins stabilize neuron structure in a BLA→PL→DMS circuit? *And in particular, during an adolescent sensitive period?* To address these questions, we integrated into our experimental design mice in which β1-integrins were lost *prior to* adolescence, to complement conditions in which β1-integrins were lost *during* or *following* adolescence. Reducing β1-integrins prior to adolescence via viral vector delivery is difficult due to the small size of neonatal mice. For example, to measure the consequences of protein loss at P21 using the same strategies that we used above, we would have needed to deliver viral vectors at P0. At that time, it would be impossible to use the same stereotactic and anesthetic approaches. Given these challenges, we instead crossed YFP + *Itgb1*-flox mice with mice expressing *Emx1*-Cre to achieve forebrain-specific loss of *Itgb1* starting at embryonic day 11.5, when the *Emx1* promoter becomes active (Gorski et al., 2002). Other groups of *Itgb1*-flox mice received either control or Cre-expressing viral vectors as in prior figures and summarized in Table 1. Thus, we were able to compare the effects of embryonic-, adolescent-, and adult-onset β1-integrin loss on layer V PL neurons, including those positioned in a BLA→PL→DMS circuit (though we did not compare across ages, due to differences in tissue preparation). A timeline reflecting gene silencing and euthanasia timing is provided in Fig. 4a.

Dendritic spine imaging and reconstruction revealed that β1-integrins in adolescence, but not earlier or later, control dendritic spine density (Fig. S3) and subtype distribution on PL neurons. Proportions of mushroom- and thin-type spines were lower in both adolescent β1-integrin-deficient conditions (i.e., general layer V neurons and those positioned in a BLA→PL→DMS circuit), and comparisons were statistically significant on projection-defined neurons [projection-defined mushroom ($t_{(11)} = 2.400$, $p = 0.04$), thin ($t_{(11)} = 2.235$, $p = 0.05$); general population mushroom ($t_{(12)} = 1.972$, $p = 0.07$), thin ($t_{(12)} = 1.948$, $p = 0.08$)] (Fig. 4b, c). β1-integrin reduction in adolescence accordingly elevated proportions of stubby-type spines, as expected
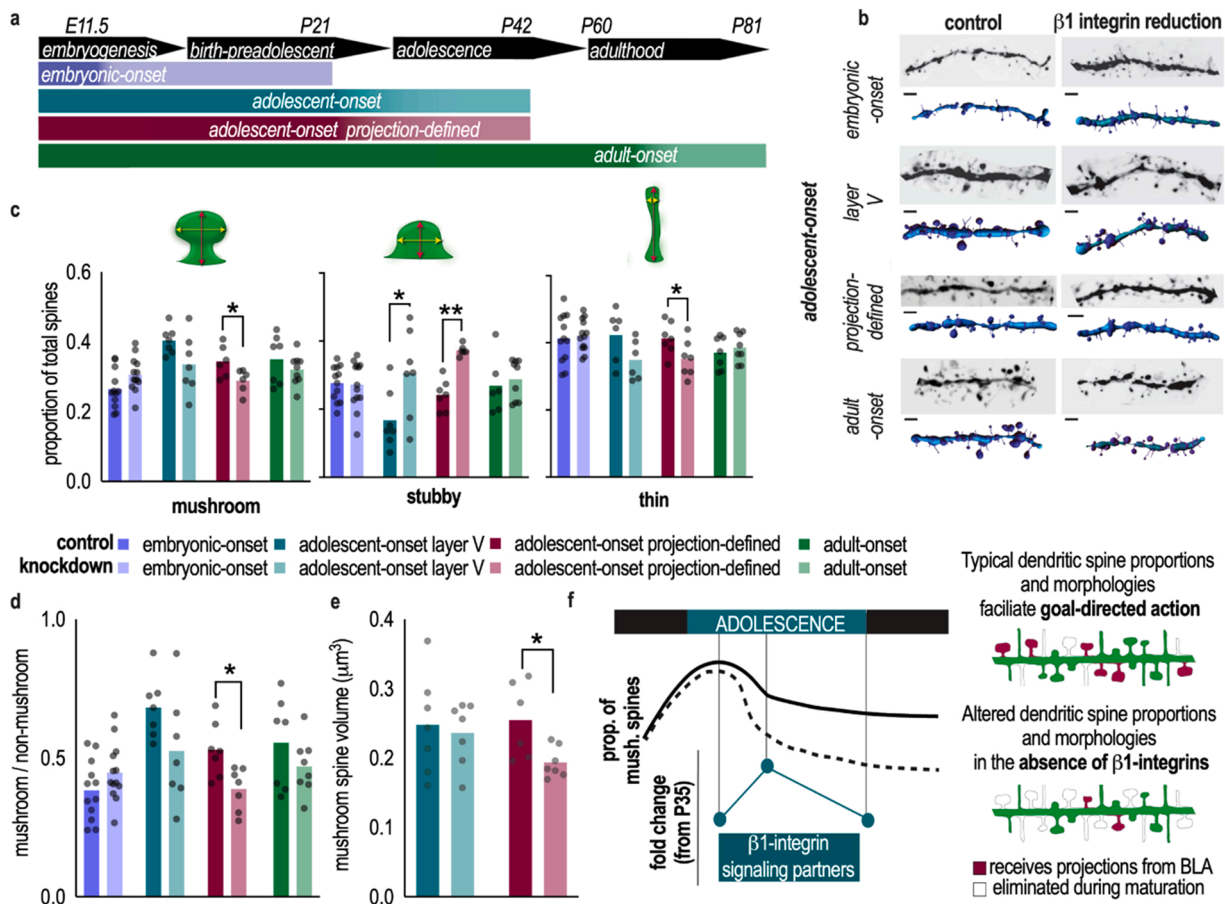

Fig. 4. Cell adhesion control of PL neuronal morphology. a. Timeline. β1-integrins were reduced starting in embryogenesis, adolescence (globally or specifically in projection-defined BLA→PL→DMS neurons), or adulthood. Timing of diminishing β1-integrin tone is represented by thinning color gradient. Dendritic spine analysis occurred at P21, P42, or P81 for embryonic-, adolescent-, or adult-onset investigations, respectively. **b.** Representative dendrites, with their associated 3D reconstructions. Scale bar = 2 μm. **c.** Adolescent-onset β1-integrin reduction decreased the proportion of mushroom- and thin-type dendritic spines and increased the proportion of stubby-type spines. Embryonic- and adult-onset β1-integrin reduction did not affect dendritic spine proportions. **d.** Adolescent-onset β1-integrin loss in projection-defined neurons decreased the proportion of mature mushroom-shaped spines to non-mushroom spines. **e.** β1-integrin tone during adolescence is also required for intact mushroom spine volume on projection-defined neurons. **f.** Model. Typical dendritic spine densities increase in the PL in the pre-adolescent period, then some dendritic spines are eliminated, and others are stabilized during adolescence. β1-integrin signaling partners increase in expression during adolescence (Shapiro et al., 2017). Here, we show that β1-integrin presence stabilizes dendritic spines on PL neurons, including neurons that receive input from the BLA and project to the DMS. Absent this activity, typical proportions and morphologies of mature, mushroom-shaped spines are lost (dashed line), and PL function is compromised in adulthood. Bars represent means. Symbols represent individual mice. *$p < 0.05$, **$p < 0.001$.

[projection-defined ($t_{(11)}$ = 6.758, p < 0.0001); general population ($t_{(12)}$ = 2.353, p = 0.04)] (Fig. 4b, c). When we calculated the proportion of mushroom to non-mushroom spines, projection-defined PL neurons again suffered a significant loss [$t_{(11)}$ = 2.745, p = 0.02], reflecting lower proportions of mature spines – those likely to contain synapses (Fig. 4d).

In contrast to the adolescent groups, embryonic-onset and adult-onset β1-integrin reduction had no effects [p > 0.05] (Fig. 4b, c), even despite gross cortical layering deficits following embryonic gene silencing (Huang et al., 2006) (Fig. S4).

Finally, we compared the volumes of dendritic spines in our adolescent groups. In addition to changing spine proportions, β1-integrin loss decreased the volumes of mature, mushroom-shaped spines on projection-defined neurons [Welch's corrected $t_{(6.408)}$ = 2.535, p = 0.04], but not in the general population [$t_{(12)}$ = 0.3584, p = 0.73] (Fig. 4e). Thus, β1-integrins sustain typical proportions and morphologies of mature, mushroom-shaped dendritic spines – those most likely to contain synapses – within a developing BLA→PL→DMS pathway (model in Fig. 4f). We posit that this function enables mature PL neurons to house stable synaptic connections necessary for adaptive action in adulthood.

3. Discussion

Across mammalian species, PFC development extends well into adolescence. Concurrent processes – dendritic spine elimination and stabilization – determine which inputs will be maintained until adulthood (Chen et al., 2014). We report that the cellular adhesion factor β1-integrin in the PL subregion of the PFC stabilizes dendritic spines on excitatory neurons during adolescent development, and adolescent β1-integrin presence is required for PL function in adulthood, specifically, in choosing actions based on their consequences. Next, we confirmed that β1-integrins are required on developing PL neurons, including on PL neurons within a projection-defined circuit, receiving projections from the BLA and projecting to the DMS, to support healthy dendritic spine micro-architecture later in life. We envision that β1-integrin-mediated dendritic spine stabilization during adolescence provides key synaptic substrates for adaptive action in adulthood.

3.1. Cell adhesion during adolescence is required for adaptive action later in life

Both humans and rodents are sensitive to the relationships between actions and their outcomes. Typical mice will change behaviors if causal relationships deteriorate, or if the value of a given outcome declines. We report that β1-integrins in the PL during adolescence are necessary for these action strategies. Specifically, reducing β1-integrins in adolescence rendered mice less likely to select actions based on likely outcomes or outcome value. Lesions and inducible inactivation of the PL have the same effects (Woon et al., 2020; Balleine and O'Doherty, 2010), but the current report is the first, to the best of our knowledge, to establish the necessity of a cell adhesion receptor in these functions. Reducing β1-integrins in adulthood had no effects; thus, it appears likely that β1-integrins support adaptive action via the stabilization of dendritic spines during adolescence, as opposed to any acute function in synaptic plasticity in adulthood. Importantly, these findings in mature mice do not negate the established function of the PL in action-outcome decision making in mature rodents; rather, they rule out β1-integrin as a major factor that controls this capacity in the post-adolescent period.

3.2. Developmental β1-integrins are necessary for the morphological features of PL neurons positioned in a BLA→PL→DMS circuit

The ability to select actions based on their consequences requires PL outputs to the DMS (Hart et al., 2018a, 2018b). Further, the ability of PL→DMS projections to exert control over adaptive action is subject to input from the BLA, as inactivation of the BLA prevents learning-related plasticity at PL→DMS synapses (Fisher et al., 2020). We thus visualized developing adolescent PL neurons positioned within this di-synaptic circuit, receiving projections from the BLA and projecting to the DMS. We enumerated: thin-type dendritic spines, which exhibit rapid turnover with a high potential for involvement in learning and memory; stubby-type dendritic spines, a transitory phenotype that does not contain synapses; and mushroom-shaped spines, which house high densities of glutamate receptors and stable synapses (Kasai et al., 2010). Interestingly, in some ways, these projection-defined adolescent PL neurons more closely resembled mature PL neurons than a general population of same-age adolescent neurons, namely the proportion of mature, mushroom-shaped spines detectable on dendrites.

One notable difference was that the mushroom-shaped spines on adult neurons were larger in volume than those on adolescent neurons, including projection-defined adolescent neurons. Larger spines are less motile and less plastic than other spines (Holtmaat et al., 2005), containing large stable synapses (Harris and Stevens, 1989) and a high density of AMPA receptors (Matsuzaki et al., 2001; Noguchi et al., 2005). In contrast, smaller dendritic spines contain relatively more NMDA receptors (Kasai et al., 2003), are highly sensitive to Ca^{2+}-mediated signaling (Nimchinsky et al., 2004), and exhibit a greater capacity for activity-dependent synaptic strengthening. Thus, adolescent neurons appear to be primed for new learning, with high densities of small mushroom-shaped spines. Reinforcement learning and the capacity for action selection according to action-outcome contingencies improve throughout adolescence (Moin Afshar et al., 2020; Naneix et al., 2012). Likely mechanistic factors driving this improvement include the strengthening of BLA→PL connectivity (Cunningham et al., 2002), the elimination of extraneous dendritic spines on PL neurons (Shapiro et al., 2017; Johnson et al., 2016), and as we reveal, the integrin-mediated maturation of dendritic spines on PL neurons receiving input from the BLA and projecting to the DMS (Fig. 4).

Due to the technical challenges of imaging projection-defined neurons, we only imaged these neurons in adolescents. In the future, analyzes of projection-defined neurons at multiple time points will shed even more comprehensive light onto BLA→PL→DMS circuit development. Also of note, our comparisons here were between projection-defined neurons and neurons that were randomly transduced by a fluorescence-expressing viral vector. Some of these randomly transduced neurons would be expected to be – by chance – positioned within a BLA→PL→DMS circuit. Thus, the reported differences here may be somewhat diluted by the inclusion of these cells. A different approach would have been to compare transduced BLA→PL→DMS circuit neurons to non-transduced neurons in the same mice. In this case, the non-transduced neurons would definitively *not* be within a BLA→PL→DMS circuit. We opted for the present approach, though, because we felt it important to control for viral vector presence.

To determine whether β1-integrin presence controlled PL neuron development during an adolescent sensitive period, we integrated into our anatomical investigation a group of mice with embryonic-onset gene silencing, to complement neurons that had undergone adolescent- or adult-onset gene silencing. Despite the inclusion of these multiple conditions, β1-integrin loss only in adolescence modified dendritic spine subtype presence, biasing dendritic spine subtypes towards stubby-type spines at the expense of mushroom- and thin-type spines (those with higher potential for synaptic presence). This effect was most profound in projection-defined neurons. Lower-than-typical proportions of mature spine types likely imperil signal fidelity from incoming projections. We posit that β1-integrin tone in adolescence confers structural stability, preserving synaptic efficacy (Matsuzaki et al., 2001; Noguchi et al., 2005). Supporting this perspective, β1-integrins signal in neurons through p190RhoGAP and ROCK2 to encourage actin filament proliferation (Sfakianos et al., 2007), thereby maintaining dendritic complexity (Warren et al., 2012), and prefrontal cortical levels of these proteins peak in adolescence (Shapiro et al., 2017). Further, β1-integrins

promote interactions between the Arp2/3 complex and cortactin, supporting actin branching and polymerization (MacGrath and Koleske, 2012; Weaver et al. 2001; Shaw et al., 2021), processes that would enable the maturation of spines from an immature to mushroom morphology capable of housing synapses. Branching and actin polymerization would also counter the retraction or elimination of mushroom-type spines. In vivo imaging could disentangle precise β1-integrin functions in developing neurons at more granular levels (e. g., see Johnson et al., 2016).

Notably, β1-integrins are involved in activity-dependent plasticity: For instance, while integrin ligands do not alter baseline physiological properties of cultured hippocampal neurons, they stabilize long-term potentiation (LTP) (Bahr et al., 1997). Further, integrin blocking anti-sera disrupts LTP-induced actin polymerization and consolidation (Kramár et al., 2006; Ackermann and Matus, 2003). Multiple aspects of dendritic spine maturation in adolescence are activity-dependent (Chen et al., 2014), thus the recruitment of β1-integrins seems sensible. Meanwhile, loss of β1-integrins *before* adolescence here had no effects on dendritic micro-architecture, even while cortical layering was profoundly disrupted (see Supplementary Fig). Similarly, β1-integrins in embryogenesis do not appear to impact dendritic spine densities on hippocampal CA1 neurons, even while they are involved in the proper maturation of presynaptic physiology (Huang et al., 2006), likely via the signaling partner talin (Morgan et al., 2004). Thus, β1-integrin function apparently depends on developmental stage. Interestingly, we found no effects of β1-integrin reduction in adulthood on dendritic spine morphologies. This outcome might highlight the exquisite capacity of cell adhesion factors to compensate for one another in mature organisms (Mortillo et al., 2012).

4. Conclusions

To summarize, we find that presence of the cell adhesion molecule β1-integrin during adolescence is essential for adaptive action later in life. Further, β1-integrins stabilize PL neurons receiving input from the BLA. These connections are integral to adaptive action (Fisher et al., 2020). Thus, it seems likely that destabilizing their capacity to house stable synapses (via β1-integrin loss) imperils the capacity of mice to select actions based on likely outcomes.

Integrin signaling is thought to be dysregulated in substance use disorders (Drgon et al., 2010) and schizophrenia (Jaffe et al., 2018), diseases that often form or first present in adolescence and in which defects in the capacity for adaptive action are hallmark. Several β1-integrin signaling partners are pharmacologically modulable, opening avenues for new clinical applications. For instance, stimulating β1-integrin-mediated signaling pathways during adolescence could potentially combat decision-making difficulties that are characteristic, and often reinforcing, of illness (Cáceda et al., 2014). More broadly, better understanding which cell adhesion molecules support adolescent brain development (and how) may prove to be fertile ground in developing new therapeutic approaches.

5. Materials and methods

5.1. Subjects

Experiments used transgenic *Itbg1*^{tm1Efu} (*Itgb1*-flox) mice bred on a mixed strain background (C57BL/6J;129X1/SvJ). These mice have loxP sites flanking exon 3 of *Itgb1*; Cre introduction deletes this exon (Raghavan et al., 2000). *Itgb1*-flox mice were crossed with mice expressing YFP under the *Thy1* gene (H line (Feng et al., 2000); back-crossed onto a C57BL/6 background) for dendritic spine imaging. For embryonic-onset *Itgb1* silencing, *Itgb1*-flox/*Thy1*-YFP mice were then crossed with mice expressing *Emx1*-Cre (back-crossed onto a C57BL/6 background). In this case, roughly 88% of neurons in the cortex and hippocampus express Cre beginning at embryonic day (E)

11.5 (Gorski et al., 2002). Mutant mice were originally purchased from Jackson Labs and then bred in-house. Both sexes were used, and we did not detect sex differences throughout. Mice were maintained on a 12 h light cycle (0700 on) and provided food and water ad libitum unless otherwise noted. Procedures were approved by the Emory University IACUC.

Table 1 summarizes the experiments in this report, including which mice were used in each experiment and ages of manipulations. For knockdown experiments, mice infused with Cre-expressing viral vectors between postnatal days (P) 21–24 are referred to as the "adolescent-onset" group because viral-mediated gene silencing would be expected to occur during adolescence, generally thought to start at P28 in rodents. Meanwhile, Cre-expressing viral vectors were delivered at or around P56 in the adult condition.

5.2. Stereotaxic surgery and viral vectors

Mice were anesthetized with ketamine/dexmedetomidine (100 mg/kg/0.5 mg/kg, intraperitoneal injection (*i.p.*)) and placed in a digitized stereotaxic frame (Stoelting). Small holes were drilled in the skull, and viral vectors were infused at AP + 1.7 mm, ML ± 0.17, DV-2.5 (PL); AP-1.4, ML ± 3.0, DV-4.9 (BLA); or AP + 0.5, ML ± 1.5, DV-4.25 (DMS). Viral vectors were infused over 5 min in a volume of 0.5 μl. Viral vectors were supplied by UNC Viral Vector Core or Addgene and are described in Table 1. Syringes were left in place for ≥ 5 min for PL infusions, or ≥ 8 min for BLA/DMS infusions, prior to removal and suturing. Mice were revived with antisedan and left undisturbed for at least 3 weeks prior to euthanasia (for immunoblotting or dendritic spine analysis) or behavioral experiments.

5.3. Immunoblotting

Mice were euthanized via rapid decapitation after brief anesthesia with isoflurane. Brains were extracted, frozen at − 80 °C, and sectioned using a chilled brain matrix into 1 mm slices. Tissue punches containing the PL were extracted using a 1 mm diameter tissue core. Tissues were homogenized in lysis buffer (200 μl: 137 mM NaCl, 20 mM tris-HCl (pH = 8), 1% igepal, 10% glycerol, 1:100 Phosphatase Inhibitor Cocktails 2 and 3 (Sigma), 1:1000 Protease Inhibitor Cocktail (Sigma)), and stored at − 80 °C. Protein concentrations were determined using a Bradford colorimetric assay kit (Pierce).

15 μg of protein was separated by SDS-PAGE on 7.5% gradient tris-glycine gels (Bio-Rad). Following transfer to PVDF membrane, blots were blocked with 5% nonfat milk for 1 h. Membranes were subsequently incubated with primary antibodies: β1-integrin (rabbit, Cell Signaling, 4706, 1:200), anti-RhoGAP p190 (mouse, Millipore, 05378, 1:1000), anti-phosphotyrosine (mouse, generously provided by A. Koleske, clone 4G10, 1:500). p190RhoGAP is the predominant phosphotyrosine-containing protein of 190 kD recognized by the 4G10 antibody in mouse brain tissue (Brouns et al., 2001) so we used the phosphotyrosine antibody to detect phosphorylated p190RhoGAP.

After exposure to primary antibodies, membranes were incubated in horseradish peroxidase secondary antibodies (anti-mouse, 1:10,000, Jackson ImmunoResearch; anti-rabbit, 1:10,000, Vector Labs) for 1 h. Immunoreactivity was assessed using a chemiluminescence substrate (Pierce) and measured using a ChemiDoc MP Imaging System (Bio-Rad). For β1-integrins, densitometry values were first normalized to a loading control, then normalized to the control sample mean from the same membrane in order to control for variance in fluorescence between gels. Phosphorylated p190RhoGAP levels were normalized to total p190RhoGAP. Immunoblots were replicated at least twice.

5.4. Instrumental response training

All mice were tested in adulthood (> P56). First, mice were food restricted to ~ 90% of their free-feeding body weight to motivate food-

reinforced responding. Mice were then trained to nose poke for 2 distinct food reinforcers (20 mg Bio-Serv Dustless Precision Pellets, grain and chocolate) in Med Associates operant conditioning chambers equipped with 2 nose poke apertures and a separate food magazine. Responding on each aperture was reinforced using a fixed ratio 1 (FR1) schedule of reinforcement, such that 30 pellets were available for responding on each aperture. Sessions ended at 70 min or 60 pellets acquired. Training ended after at least 7 sessions, when mice acquired all 60 pellets within 70 min. Response acquisition curves represent responses/min for both nose poke apertures during the last 7 training sessions, with no side or pellet preferences throughout.

Test for action-outcome response selection was used as previously described (DePoy et al., 2019; Gourley et al., 2012). First, 1 of the 2 apertures was available, and responding continued to be reinforced according to an FR1 schedule for 25 min. As such, the action-outcome contingency associated with that aperture remained intact. The following day, the other aperture was available for a 25 min session during which the action-outcome association between that nose poke behavior and reward were violated. In this case, pellets were delivered non-contingently at a rate matched to each animal's reinforcement rate from the previous session. Responding was not reinforced, uncoupling the response-pellet relationship (Butkovich et al., 2015). Thus, this nose poke action becomes significantly less predictive of reinforcement than the other. The apertures, as well as the order of the "non-contingent" and "contingent" sessions, were counterbalanced.

Finally, both apertures were made available during a 15 min probe test conducted in extinction the following day. Preferential engagement of the response that remained reinforced is evidence of using causal knowledge to guide choice.

5.5. Outcome devaluation

A version of classical instrumental outcome devaluation was used, as previously described (Balleine et al., 2003). Following response training, mice were placed into a clean, novel chamber with 1–2 g of either grain- or chocolate-flavored pellets for 30 min (males) or 90 min (females), devaluing that pellet. (In our experience, females require longer to consume this amount, hence the longer prefeeding period.) Immediately following, mice were placed in the operant conditioning chambers, and both apertures were available for a 15 min probe test conducted in extinction. Action selection according to outcome value is reflected by preferential responding for the valued relative to devalued pellet. If mice ate < 0.3 g during the prefeeding period, the procedure was repeated.

5.6. Histology

Mice were euthanized and sections collected as described for dendritic spine imaging below. The mCherry tag was visualized. Immunohistochemistry for mCherry (mouse, 1:1000, Takara; goat anti-mouse-alexa594, 1:500, Invitrogen) was used to delineate viral vector spread, as needed.

5.7. Dendritic spine imaging

Mice were euthanized by rapid decapitation after brief anesthesia with isoflurane, and brains were extracted and submerged in 4% paraformaldehyde. For analysis of viral vector transfection, mice were transcardially perfused under deep anesthesia with ketamine/xylazine (120 mg/kg/10 mg/kg), prior to brain incubation in 4% paraformaldehyde. Brains were next transferred to 30% w/v sucrose solution, then were sectioned on a Leica microtome held at − 15 °C into 50 μm sections, mounted, and coverslipped. Unobstructed dendritic segments co-expressing mCherry and YFP were imaged on a spinning disk confocal (VisiTech International) on a Leica DM 5500B microscope. Z-stacks were collected with a 100 × 1.4NA objective using a 0.1 μm step size, sampling above and below the dendrite. After imaging, we

confirmed at 10 × that the image was collected from the PL. For each animal, 5–12 independent basal dendrite segments, located 25–150 μm from the soma, were imaged.

Dendritic spines were reconstructed in 3-D using Imaris software and previously described methods (Gourley et al., 2013). Each experiment was scored by a single blinded rater. Each protrusion ≤ 4.5 μm in length was considered a spine. Bifurcated spines were considered singular units. Dendritic spines less than 0.6 μm in length were defined as stubby. If spine length was greater than 0.6 μm, spine classification was dependent on head diameter: spines with a head diameter more than 2 times the neck diameter were classified as mushroom, and spines with a head diameter less than 2 times the neck diameter were classified as thin (Cooper and Koleske, 2014).

5.8. Statistics

All statistics were performed using GraphPad Prism and SPSS. Immunoblotting results were analyzed using a 2-tailed, unpaired t-test and 1-sample t-tests against 1, as indicated. Repeating measures (RM) ANOVAs were used to compare response rates in the behavioral experiments. Tukey's post-hoc tests were used in the case of significant interactions or main effects with > 2 groups and are indicated in the figures. Values > 2 standard deviations above the mean were considered outliers and excluded.

Proportions of each dendritic spine subtype were generated by dividing a given spine subtype number by the total spine number for that dendritic segment. For dendritic spine subtype proportion and morphometric analyses, each animal contributed one value reflecting the average of its dendrites. For initial subtype and morphometric comparisons, a 1-way ANOVA was used. Any significant effects were explored using Tukey's post-hoc analyses. In the case of unequal variances, as analyzed by a Brown-Forsythe test, a Welch's ANOVA was used instead, with Dunnett T3 post-hocs. Knockdown comparisons were analyzed using 2-tailed, unpaired t-tests.

Appendix A. Supporting information

Supplementary data associated with this article can be found in the online version at doi:10.1016/j.dcn.2022.101097.

References

Ackermann, M., Matus, A., 2003. Activity-induced targeting of profilin and stabilization of dendritic spine morphology. Nat. Neurosci. 6 (11), 1194–1200. https://doi.org/10.1038/nn1135.

Moin Afshar, N., Keip, A.J., Taylor, J.R., Lee, D., Groman, S.M., 2020. Reinforcement learning during adolescence in rats. J. Neurosci. 40 (30), 5857–5870. https://doi.org/10.1523/jneurosci.0910-20.2020 (PubMed PMID: 32601244; PMCID: PMC7380962).

Ahmed, B.Y., Chakravarthy, S., Eggers, R., Hermens, W.T., Zhang, J.Y., Niclou, S.P., Levelt, C., Sablitzky, F., Anderson, P.N., Lieberman, A.R., Verhaagen, J., 2004. Efficient delivery of Cre-recombinase to neurons in vivo and stable transduction of neurons using adeno-associated and lentiviral vectors. BMC Neurosci. 5 (1), 4. https://doi.org/10.1186/1471-2202-5-4.

Bahr, B.A., Staubli, U., Xiao, P., Chun, D., Ji, Z.X., Esteban, E.T., Lynch, G., 1997. Arg-Gly-Asp-Ser-selective adhesion and the stabilization of long-term potentiation: pharmacological studies and the characterization of a candidate matrix receptor. J. Neurosci.: Off. J. Soc. Neurosci. 17 (4), 1320–1329. https://doi.org/10.1523/JNEUROSCI.17-04-01320.1997 (PubMed PMID: 9006975).

Balleine, B.W., Killcross, A.S., Dickinson, A., 2003. The effect of lesions of the basolateral amygdala on instrumental conditioning. J. Neurosci.: Off. J. Soc. Neurosci. 23 (2), 666–675. https://doi.org/10.1523/JNEUROSCI.23-02-00666.2003 (PubMed PMID: 12533626).

Balleine, B.W., O'Doherty, J.P., 2010. Human and rodent homologies in action control: corticostriatal determinants of goal-directed and habitual action. Neuropsychopharmacology 35 (1), 48–69. https://doi.org/10.1038/npp.2009.131 (PubMed PMID: PMC3055420).

Bradley, W.D., Hernández, S.E., Settleman, J., Koleske, A.J., 2006. Integrin signaling through Arg activates its binding to p120RasGAP and recruitment to the membrane. Mol. Biol. Cell 17 (11), 4827–4836.

Brouns, M.R., Matheson, S.F., Settleman, J., 2001. p190 RhoGAP is the principal Src substrate in brain and regulates axon outgrowth, guidance and fasciculation. Nat. Cell Biol. 3 (4), 361–367. https://doi.org/10.1038/35070042 (PubMed PMID: 11283609).

Butkovich, L.M., DePoy, L.M., Allen, A.G., Shapiro, L.P., Swanson, A.M., Gourley, S.L., 2015. Adolescent-onset GABAA α1 silencing regulates reward-related decision making. Eur. J. Neurosci. 42 (4), 2114–2121. https://doi.org/10.1111/ejn.12995 (PubMed PMID: 26096050).

Cáceda, R., Nemeroff, C.B., Harvey, P.D., 2014. Toward an understanding of decision making in severe mental illness. J. Neuropsychiatry Clin. Neurosci. 26 (3), 196–213. https://doi.org/10.1176/appi.neuropsych.12110268.

Cahoy, J.D., Emery, B., Kaushal, A., Foo, L.C., Zamanian, J.L., Christopherson, K.S., Xing, Y., Lubischer, J.L., Krieg, P.A., Krupenko, S.A., Thompson, W.J., Barres, B.A., 2008. A transcriptome database for astrocytes, neurons, and oligodendrocytes: a new resource for understanding brain development and function. J. Neurosci. 28 (1), 264. https://doi.org/10.1523/JNEUROSCI.4178-07.2008.

Chen, C.-C., Lu, J., Zuo, Y., 2014. Spatiotemporal dynamics of dendritic spines in the living brain. Front. Neuroanat. 8 https://doi.org/10.3389/fnana.2014.00028 (28-. PubMed PMID: 24847214).

Cheriyan, J., Kaushik, M.K., Ferreira, A.N., Sheets, P.L., 2016. Specific targeting of the basolateral amygdala to projectionally defined pyramidal neurons in prelimbic and infralimbic cortex. eNeuro 3 (2). https://doi.org/10.1523/ENEURO.0002-16.2016 (ENEURO.0002-16.2016, PubMed PMID: 27022632).

Cooper, M.A., Koleske, A.J., 2014. Ablation of ErbB4 from excitatory neurons leads to reduced dendritic spine density in mouse prefrontal cortex. J. Comp. Neurol. 522 (14), 3351–3362. https://doi.org/10.1002/cne.23615 (PubMed PMID: 24752666; PMCID: PMC4107058).

Crews, F., He, J., Hodge, C., 2007. Adolescent cortical development: a critical period of vulnerability for addiction. Pharmacol. Biochem. Behav. 86 (2), 189–199. https://doi.org/10.1016/j.pbb.2006.12.001.

Cunningham, M.G., Bhattacharyya, S., Benes, F.M., 2002. Amygdalo-cortical sprouting continues into early adulthood: implications for the development of normal and abnormal function during adolescence. J. Comp. Neurol. 453 (2), 116–130. https://doi.org/10.1002/cne.10376.

DePoy, L.M., Shapiro, L.P., Kietzman, H.W., Roman, K.M., Gourley, S.L., 2019. β1-integrins in the developing orbitofrontal cortex are necessary for expectancy updating in mice. J. Neurosci. https://doi.org/10.1523/jneurosci.3072-18.2019 (3072-18).

Drgon, T., Zhang, P.-W., Johnson, C., Walther, D., Hess, J., Nino, M., Uhl, G.R., 2010. Genome wide association for addiction: replicated results and comparisons of two analytic approaches. PLoS One 5 (1). https://doi.org/10.1371/journal.pone.0008832 (e8832-e8832. PubMed PMID: 20098672).

Feng, G., Mellor, R.H., Bernstein, M., Keller-Peck, C., Nguyen, Q.T., Wallace, M., Nerbonne, J.M., Lichtman, J.W., Sanes, J.R., 2000. Imaging neuronal subsets in transgenic mice expressing multiple spectral variants of GFP. Neuron 28 (1), 41–51. https://doi.org/10.1016/S0896-6273(00)00084-2.

Fisher, S.D., Ferguson, L.A., Bertran-Gonzalez, J., Balleine, B.W., 2020. Amygdala-cortical control of striatal plasticity drives the acquisition of goal-directed action. Curr. Biol. 30 (22), 4541–4546. https://doi.org/10.1016/j.cub.2020.08.090 (.e5).

Glausier, J.R., Lewis, D.A., 2013. Dendritic spine pathology in schizophrenia. Neuroscience 251, 90–107. https://doi.org/10.1016/j.neuroscience.2012.04.044 (PubMed PMID: PMC3413758).

Gorski, J.A., Talley, T., Qiu, M., Puelles, L., Rubenstein, J.L.R., Jones, K.R., 2002. Cortical excitatory neurons and glia, but not GABAergic neurons, are produced in the Emx1-expressing lineage. J. Neurosci. 22 (15), 6309.

Gourley, S.L., Swanson, A.M., Jacobs, A.M., Howell, J.L., Mo, M., DiLeone, R.J., Koleske, A.J., Taylor, J.R., 2012. Action control is mediated by prefrontal BDNF and glucocorticoid receptor binding. Proc. Natl. Acad. Sci. USA 109 (50), 20714–20719. https://doi.org/10.1073/pnas.1208342109 (PubMed PMID: PMC3528547).

Gourley, S.L., Swanson, A.M., Koleske, A.J., 2013. Corticosteroid-induced neural remodeling predicts behavioral vulnerability and resilience. J. Neurosci. 33 (7), 3107–3112. https://doi.org/10.1523/jneurosci.2138-12.2013 (PubMed PMID: 23407565; PMCID: PMC3711631).

Harris, K.M., Stevens, J.K., 1989. Dendritic spines of CA 1 pyramidal cells in the rat hippocampus: serial electron microscopy with reference to their biophysical characteristics. J. Neurosci.: Off. J. Soc. Neurosci. 9 (8), 2982–2997. https://doi.org/10.1523/JNEUROSCI.09-08-02982.1989 (PubMed PMID: 2769375).

Hart, G., Bradfield, L.A., Balleine, B.W., 2018. Prefrontal corticostriatal disconnection blocks the acquisition of goal-directed action. J. Neurosci. 38 (5), 1311–1322. https://doi.org/10.1523/jneurosci.2850-17.2017.

Hart, G., Bradfield, L.A., Fok, S.Y., Chieng, B., Balleine, B.W., 2018b. The bilateral prefronto-striatal pathway is necessary for learning new goal-directed actions. Curr. Biol. 28 (14), 2218–2229. https://doi.org/10.1016/j.cub.2018.05.028 (.e7).

Hart, G., Leung, B.K., Balleine, B.W., 2014. Dorsal and ventral streams: the distinct role of striatal subregions in the acquisition and performance of goal-directed actions. Neurobiol. Learn. Mem. 108, 104–118. https://doi.org/10.1016/j.nlm.2013.11.003 (PubMed PMID: 24231424).

Holtmaat, A.J., Trachtenberg, J.T., Wilbrecht, L., Shepherd, G.M., Zhang, X., Knott, G.W., Svoboda, K., 2005. Transient and persistent dendritic spines in the neocortex in vivo. Neuron 45 (2), 279–291. https://doi.org/10.1016/j.neuron.2005.01.003 (PubMed PMID: 15664179).

Huang, Z., Shimazu, K., Woo, N.H., Zang, K., Müller, U., Lu, B., Reichardt, L.F., 2006. Distinct roles of the β1-class integrins at the developing and the mature hippocampal excitatory synapse. J. Neurosci.: Off. J. Soc. Neurosci. 26 (43), 11208–11219. https://doi.org/10.1523/JNEUROSCI.3526-06.2006 (PubMed PMID: PMC2693048).

Humphrey, J.D., Dufresne, E.R., Schwartz, M.A., 2014. Mechanotransduction and extracellular matrix homeostasis. Nat. Rev. Mol. Cell Biol. 15 (12), 802–812. https://doi.org/10.1038/nrm3896 (PubMed PMID: 25355505).

Ivankovic-Dikic, I., Gronroos, E., Blaukat, A., Barth, B.-U., Dikic, I., 2000. Pyk2 and FAK regulate neurite outgrowth induced by growth factors and integrins. Nat. Cell Biol. 2 (9), 574–581.

Jaffe, A.E., Straub, R.E., Shin, J.H., Tao, R., Gao, Y., Collado-Torres, L., Kam-Thong, T., Xi, H.S., Quan, J., Chen, Q., Colantuoni, C., Ulrich, W.S., Maher, B.J., Deep-Soboslay, A., Cross, A.J., Brandon, N.J., Leek, J.T., Hyde, T.M., Kleinman, J.E., Weinberger, D.R., 2018. Developmental and genetic regulation of the human cortex transcriptome illuminate schizophrenia pathogenesis. Nat. Neurosci. 21 (8), 1117–1125. https://doi.org/10.1038/s41593-018-0197-y.

Johnson, C.M., Loucks, F.A., Peckler, H., Thomas, A.W., Janak, P.H., Wilbrecht, L., 2016. Long-range orbitofrontal and amygdala axons show divergent patterns of maturation in the frontal cortex across adolescence. Dev. Cogn. Neurosci. 18, 113–120. https://doi.org/10.1016/j.dcn.2016.01.005.

Kasai, H., Fukuda, M., Watanabe, S., Hayashi-Takagi, A., Noguchi, J., 2010. Structural dynamics of dendritic spines in memory and cognition. Trends Neurosci. 33 (3), 121–129. https://doi.org/10.1016/j.tins.2010.01.001.

Kasai, H., Matsuzaki, M., Noguchi, J., Yasumatsu, N., Nakahara, H., 2003. Structure-stability-function relationships of dendritic spines. Trends Neurosci. 26 (7), 360–368. https://doi.org/10.1016/s0166-2236(03)00162-0 (PubMed PMID: 12850432).

Kessler, R.C., Angermeyer, M., Anthony, J.C., De Graaf, R., Demyttenaere, K., Gasquet, I., De Girolamo, G., Gluzman, S., Gureje, O., Haro, J.M., Kawakami, N., Karam, A., Levinson, D., Medina Mora, M.E., Oakley Browne, M.A., Posada-Villa, J., Stein, D.J., Adley Tsang, C.H., Aguilar-Gaxiola, S., Alonso, J., Lee, S., Heeringa, S., Pennell, B.-E., Berglund, P., Gruber, M.J., Petukhova, M., Chatterji, S., Ustün, T.B., 2007. Lifetime prevalence and age-of-onset distributions of mental disorders in the World Health Organization's World Mental Health Survey Initiative. World Psychiatry 6 (3), 168–176 (PubMed PMID: 18188442).

Kramár, E.A., Lin, B., Rex, C.S., Gall, C.M., Lynch, G., 2006. Integrin-driven actin polymerization consolidates long-term potentiation. Proc. Natl. Acad. Sci. USA 103 (14), 5579–5584. https://doi.org/10.1073/pnas.0601354103.

MacDonald, M.L., Alhassan, J., Newman, J.T., Richard, M., Gu, H., Kelly, R.M., Sampson, A.R., Fish, K.N., Penzes, P., Wills, Z.P., Lewis, D.A., Sweet, R.A., 2017. Selective loss of smaller spines in schizophrenia. Am. J. Psychiatry 174 (6), 586–594. https://doi.org/10.1176/appi.ajp.2017.16070814.

MacGrath, S.M., Koleske, A.J., 2012. Arg/Abl2 modulates the affinity and stoichiometry of binding of cortactin to F-actin. Biochemistry 51 (33), 6644–6653. https://doi.org/10.1021/bi300722t (PubMed PMID: PMC3556572).

Matsuzaki, M., Ellis-Davies, G.C., Nemoto, T., Miyashita, Y., Iino, M., Kasai, H., 2001. Dendritic spine geometry is critical for AMPA receptor expression in hippocampal CA1 pyramidal neurons. Nat. Neurosci. 4 (11), 1086–1092. https://doi.org/10.1038/nn736 (PubMed PMID: 11687814).

Morgan, J.R., Di Paolo, G., Werner, H., Shchedrina, V.A., Pypaert, M., Pieribone, V.A., De Camilli, P., 2004. A role for talin in presynaptic function. J. Cell Biol. 167 (1), 43–50. https://doi.org/10.1083/jcb.200406020 (PubMed PMID: 15479735).

Mortillo, S., Elste, A., Ge, Y., Patil, S.B., Hsiao, K., Huntley, G.W., Davis, R.L., Benson, D. L., 2012. Compensatory redistribution of neuroligins and N-cadherin following deletion of synaptic β1-integrin. J. Comp. Neurol. 520 (9), 2041–2052. https://doi.org/10.1002/cne.23027 (PubMed PMID: 22488504; PMCID: PMC3496382).

Naneix, F., Marchand, A.R., Di Scala, G., Pape, J.-R., Coutureau, E., 2012. Parallel maturation of goal-directed behavior and dopaminergic systems during adolescence. J. Neurosci.: Off. J. Soc. Neurosci. 32 (46), 16223–16232. https://doi.org/10.1523/JNEUROSCI.3080-12.2012 (PubMed PMID: 23152606).

Nimchinsky, E.A., Yasuda, R., Oertner, T.G., Svoboda, K., 2004. The number of glutamate receptors opened by synaptic stimulation in single hippocampal spines. J. Neurosci. 24 (8), 2054–2064. https://doi.org/10.1523/jneurosci.5066-03.2004 (PubMed PMID: 14985448; PMCID: PMC6730404).

Noguchi, J., Matsuzaki, M., Ellis-Davies, G.C., Kasai, H., 2005. Spine-neck geometry determines NMDA receptor-dependent Ca^{2+} signaling in dendrites. Neuron 46 (4), 609–622. https://doi.org/10.1016/j.neuron.2005.03.015 (PubMed PMID: 15944129; PMCID: PMC4151245).

Pasterkamp, R.J., Peschon, J.J., Spriggs, M.K., Kolodkin, A.L., 2003. Semaphorin 7A promotes axon outgrowth through integrins and MAPKs. Nature 424 (6947), 398–405. https://doi.org/10.1038/nature01790.

Penzes, P., Cahill, M.E., Jones, K.A., VanLeeuwen, J.-E., Woolfrey, K.M., 2011. Dendritic spine pathology in neuropsychiatric disorders. Nat. Neurosci. 14 (3), 285–293. https://doi.org/10.1038/nn.2741 (PubMed PMID: PMC3530413).

Raghavan, S., Bauer, C., Mundschau, G., Li, Q., Fuchs, E., 2000. Conditional ablation of beta1 integrin in skin. Severe defects in epidermal proliferation, basement membrane formation, and hair follicle invagination. J. Cell Biol. 150 (5), 1149–1160. https://doi.org/10.1083/jcb.150.5.1149 (PubMed PMID: 10974002).

Rosen, GD, Williams, A.G., Capra, J.A., Connolly, M.T., Cruz, B., Lu, L., Airey, D.C., Kulkarn, i.K., Williams, R.W., 2000. The mouse brain library @ ⟨www.mbl.org⟩. In: Proceedings of the Int Mouse Genome Conference, vol. 14(166).

Schuster, T., Krug, M., Stalder, M., Hackel, N., Gerardy-Schahn, R., Schachner, M., 2001. Immunoelectron microscopic localization of the neural recognition molecules L1, NCAM, and its isoform NCAM180, the NCAM-associated polysialic acid, beta1 integrin and the extracellular matrix molecule tenascin-R in synapses of the adult rat hippocampus. J. Neurobiol. 49 (2), 142–158. https://doi.org/10.1002/neu.1071 (PubMed PMID: 11598921).

Sfakianos, M.K., Eisman, A., Gourley, S.L., Bradley, W.D., Scheetz, A.J., Settleman, J., Taylor, J.R., Greer, C.A., Williamson, A., Koleske, A.J., 2007. Inhibition of Rho via Arg and p190RhoGAP in the postnatal mouse hippocampus regulates dendritic spine maturation, synapse and dendrite stability, and behavior. J. Neurosci. 27 (41), 10982.

Shapiro, L.P., Parsons, R.G., Koleske, A.J., Gourley, S.L., 2017. Differential expression of cytoskeletal regulatory factors in the adolescent prefrontal cortex: implications for cortical development. J. Neurosci. Res. 95 (5), 1123–1143. https://doi.org/10.1002/jnr.23960 (PubMed PMID: 27735056; PMCID: PMC5352542).

Shaw, J.E., Kilander, M.B.C., Lin, Y.C., Koleske, A.J., 2021. Abl2:cortactin interactions regulate dendritic spine stability via control of a stable filamentous actin pool. J. Neurosci. https://doi.org/10.1523/jneurosci.2472-20.2021 (PubMed PMID: 33622779).

Spear, L.P., 2000. The adolescent brain and age-related behavioral manifestations. Neurosci. Biobehav. Rev. 24 (4), 417–463. https://doi.org/10.1016/S0149-7634 (00)00014-2.

Warren, M.S., Bradley, W.D., Gourley, S.L., Lin, Y.-C., Simpson, M.A., Reichardt, L.F., Greer, C.A., Taylor, J.R., Koleske, A.J., 2012. Integrin β1 signals through Arg to regulate postnatal dendritic arborization, synapse density, and behavior. J. Neurosci. 32 (8), 2824–2834. https://doi.org/10.1523/JNEUROSCI.3942-11.2012 (PubMed PMID: PMC3313657).

Wassum, K.M., Izquierdo, A., 2015. The basolateral amygdala in reward learning and addiction. Neurosci. Biobehav. Rev. 57, 271–283. https://doi.org/10.1016/j.neubiorev.2015.08.017 (PubMed PMID: 26341938).

Weaver, A.M., Karginov, A.V., Kinley, A.W., Weed, S.A., Li, Y., Parsons, J.T., Cooper, J. A., 2001. Cortactin promotes and stabilizes Arp2/3-induced actin filament network formation. Curr. Biol., vol. 11(5), pp. 370–4. ⟨https://doi.org/10.1016/S0960-9822 (01)00098-7⟩.

Woon, E.P., Sequeira, M.K., Barbee, B.R., Gourley, S.L., 2020. Involvement of the rodent prelimbic and medial orbitofrontal cortices in goal-directed action: a brief review. J. Neurosci. Res. 98 (6), 1020–1030. https://doi.org/10.1002/jnr.24567.